Published August 15, 2005



# Intraflagellar transport (IFT) during assembly and disassembly of *Chlamydomonas* flagella

William Dentler

Department of Molecular Biosciences, University of Kansas, Lawrence, KS 66049

Intraflagellar transport (IFT) of particles along flagellar microtubules is required for the assembly and maintenance of eukaryotic flagella and cilia. In *Chlamydomonas*, anterograde and retrograde particles viewed by light microscopy average 0.12-μm and 0.06-μm diameter, respectively. Examination of IFT particle structure in growing flagella by electron microscopy revealed similar size aggregates composed of small particles linked to each other and to the membrane and microtubules. To determine the relationship between the number of particles and flagellar length, the rate and frequency of IFT particle movement was measured in nongrowing, growing, and shortening flagella. In all flagella, anterograde and retrograde IFT averaged 1.9 μm/s and 2.7 μm/s, respectively, but retrograde IFT was significantly slower in flagella shorter than 4 μm. The number of flagellar IFT particles was not fixed, but depended on flagellar length. Pauses in IFT particle entry into flagella suggest the presence of a periodic "gate" that permits up to 4 particles/s to enter a flagellum.

## Introduction

Cilia and eukaryotic flagella are microtubule-containing organelles that project from the surfaces of many eukaryotic cells. Motile cilia are widely recognized for their roles in protozoan and sperm motility, for mucus transport over oviduct and respiratory cell surfaces (Dentler, 1987), and for embryonic tissue morphogenesis (Nonaka et al., 1998; Pazour and Rosenbaum, 2002; Nauli et al., 2003; Pazour and Witman, 2003; Snell et al., 2004). Nonmotile sensory cilia detect fluid flow over endothelial cells (Praetorius et al., 2003; Iomini et al., 2004). Typical flagella are composed of a microtubular axoneme, and both the assembly and turnover of microtubule protein occur at the distal tip (Gorovsky et al., 1970; Johnson and Rosenbaum, 1992; Stephens, 2000; Song and Dentler, 2001). Microtubule disassembly is less well understood and may occur at either the distal or proximal ends (Stephens, 2000; Parker and Quarmby, 2003). Flagellar length is determined by the microtubules, but within an axoneme examples of precisely regulated lengths of individual A, B, and central microtubules occur (Dentler, 1981, 1987, 1990). The regulation individual microtubule lengths may be a property of the caps that link the A and central microtubules to the membrane (Dentler, 1980, 1981; LeCluyse and Dentler, 1984), and the length of the entire cilium may be regulated by protein kinases (Pan et al., 2004) or by a family of LF proteins that reside in the cell body (Barsel et al., 1988; Asleson and Lefebvre, 1998; Berman et al., 2003; Tam et al., 2003; Nguyen et al., 2005).

Flagellar assembly and maintenance requires intraflagellar transport (IFT) (Kozminski et al., 1993, 1995). In most cilia, heterotrimeric kinesin-2 is responsible for the anterograde movement of IFT particles to the flagellar tips, and cytoplasmic dynein mediates the transport of particles to the flagellar base. If either the motors or associated proteins are disrupted, flagella either fail to assemble or, in temperature-sensitive mutants, flagellar microtubules disassemble at restrictive temperatures (Kozminski et al., 1995; Cole et al., 1998; Pazour et al., 1998; 1999; Porter et al., 1999; Marshall and Rosenbaum, 2001; Cole, 2003; Scholey, 2003; Snow et al., 2004). Using a novel kymographic method, IFT particles were discovered to undergo nearly continuous movement up and down flagella (Iomini et al., 2001).

Although the importance of IFT for flagellar assembly is well established, its role in flagellar length regulation is not understood. Based on an immunological analysis of IFT proteins, an "equilibrium balance" model in which the number of IFT particles in a flagellum is fixed and their rate or frequency of movement regulates flagellar length was proposed (Marshall and Rosenbaum, 2001; Marshall, 2002; Marshall et al., 2005). This model predicts that either the frequency of IFT particles that enter flagella or the rates at which IFT particles move must decrease as flagellar length increases and must increase as flagella shorten. In cells with equal length flagella, the number and frequency of IFT particles should be identical, but in cells

Correspondence to William Dentler: wdent@ku.edu

Abbreviations used in this paper: DIC, differential interference contrast; IFT, intraflagellar transport.


The Journal of Cell Biology, Vol. 170, No. 4, August 15, 2005 649–659
http://www.jcb.org/cgi/doi/10.1083/jcb.200412021

Published August 15, 2005

with unequal length flagella the longer flagellum should have fewer IFT particles than does the shorter flagellum.

To test this hypothesis, the rate and frequency of IFT particle movement was examined in steady-state, growing, and disassembling flagella on *Chlamydomonas* cells. Flagella on three mutants with paralyzed flagella, two with abnormally long flagella, and one with unequal length flagella and bulbous, IFT particle-filled tips (Ulf mutant) were examined to determine the following questions. (1) Does the rate of anterograde and retrograde IFT change as a function of flagellar length? (2) Is IFT continuous or do particles start and stop within the flagellum? (3) Does the frequency or periodicity of IFT particle entry into flagella change as a function of flagellar length? (4) Is the movement of IFT particles coordinated in the two flagella on a single cell? (5) Is the rate or frequency of IFT affected if IFT particles are abnormally accumulated at the tip of a flagellum?

The results revealed that (a) the rate of IFT is nearly constant and, with the exception of very short flagella, is independent of flagellar length; (b) IFT particle entry into flagella is periodic, but gap or pauses in particle entry occurred; (c) gaps in particle entry are not coordinated between the two flagella on a single cell; and (d) accumulations of IFT particles at flagellar tips have little effect on the rate or frequency of IFT particle transport.

Based on the widths of kymograph tracks, the diameter of anterograde and retrograde particles were 0.12 μm and 0.06 μm, respectively. Similar sized aggregates of smaller particles attached to both the microtubules and the flagellar membrane were observed in thin-sectioned flagella. When examined by negative staining, the IFT particles were found to be formed by smaller particles linked by filaments. The IFT particles are linked to microtubules by discrete structures that may be the motor proteins.

## Results

### Three different anterograde and retrograde tracks are present in flagella

The movement of IFT particles was visualized using a modification of the kymograph method developed by Piperno et al. (1998). The pattern of IFT particle movement in a single *Chlamydomonas* flagellum is shown in Fig. 1 A. For most kymographs shown here, the entire flagellum is shown for a 40-s period. IFT particles are visible throughout the flagellum, although the refraction of the cell body makes it difficult to observe regions closest to the cell bodies. Because the depth of focus of the 100× NA 1.4 lens at the wavelength used was ~0.3 μm, most or all particle movement within a 0.2-μm-diameter flagellum should be visible in these micrographs.

The width of individual anterograde and retrograde particle tracks remained constant throughout the length of the flagellum. Anterograde tracks were approximately twice the width of retrograde tracks. Some variation in the thickness of tracks was observed (Fig. 1 B), and occasionally tracks appeared to merge, although close examination of the tracks suggested that the particles overlapped rather than merged, as if they were moving along different microtubules (Fig. 1 C). Some particles appeared to reverse direction before reaching the distal tip (Fig. 1 B), but most tracks extended entirely to the tip or base.

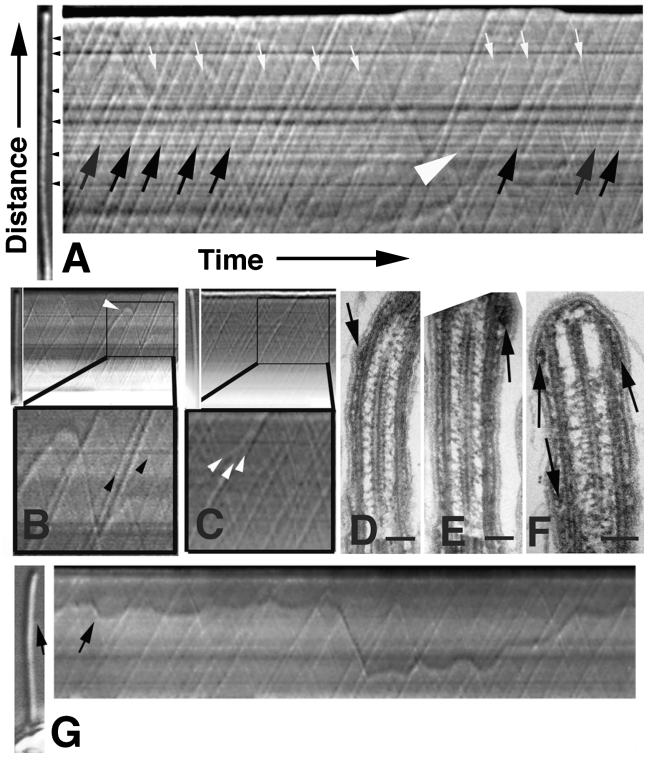


Figure 1. **Kymograph analysis of IFT particle movement.** At the left of A is a single image of a flagellum showing IFT particle "bulges" (arrowheads). The distal tip of this flagellum (and all others in this report) is at the top and the cell body is at the bottom. Movements of IFT particles were recorded and individual flagellar images were projected to produce the kymogram (right). Individual flagella are not visible, but IFT particles and their movements produce particle tracks. Movements of large IFT particles in the anterograde direction (base to tip, black arrows) and movements of smaller particles in the retrograde direction (tip to base, white arrows) are shown. Tracks of very large, slowly moving particles (white arrowhead) may be extraflagellar particles (see G). (B and C) Two flagella (left) and IFT tracks (right panels) with magnified images (insets). Most particle tracks extend completely to the tip of the flagellum but some (B, white arrowhead) appear to reverse direction without reaching the tip. Two different-size anterograde particles can be identified (B, black arrowheads) and closely spaced but not merging tracks also can be identified in C (arrowheads). (D–F) TEM images showing IFT particles in typical *Chlamydomonas* flagella. Near the tips, the large aggregates appear to become extended series of particles (arrows). Bars, 100 nm. (G) Movement of a large extraflagellar particle (arrows) superimposed on anterograde and retrograde particle tracks. The extraflagellar particle reversibly moves along the flagellum and rarely moves completely to the tip or base.

In some flagella, tracks of larger particles moved more irregularly and with significantly slower velocity than the smaller particles (Fig. 1, A and G). These particles oscillated back and forth along the flagellum, paused often, and occasionally made extended tracks. Rarely did the tracks extend completely to the flagellar tip or flagellar base. This motility is clearly different from the more regular patterns of IFT particle movement, and probably reflects extraflagellar movement of particles first described by Bloodgood (1977).

### IFT particle structure and association with microtubules and membranes

The size of IFT particles was estimated by measuring the width of anterograde and retrograde particle tracks. Anterograde

Published August 15, 2005

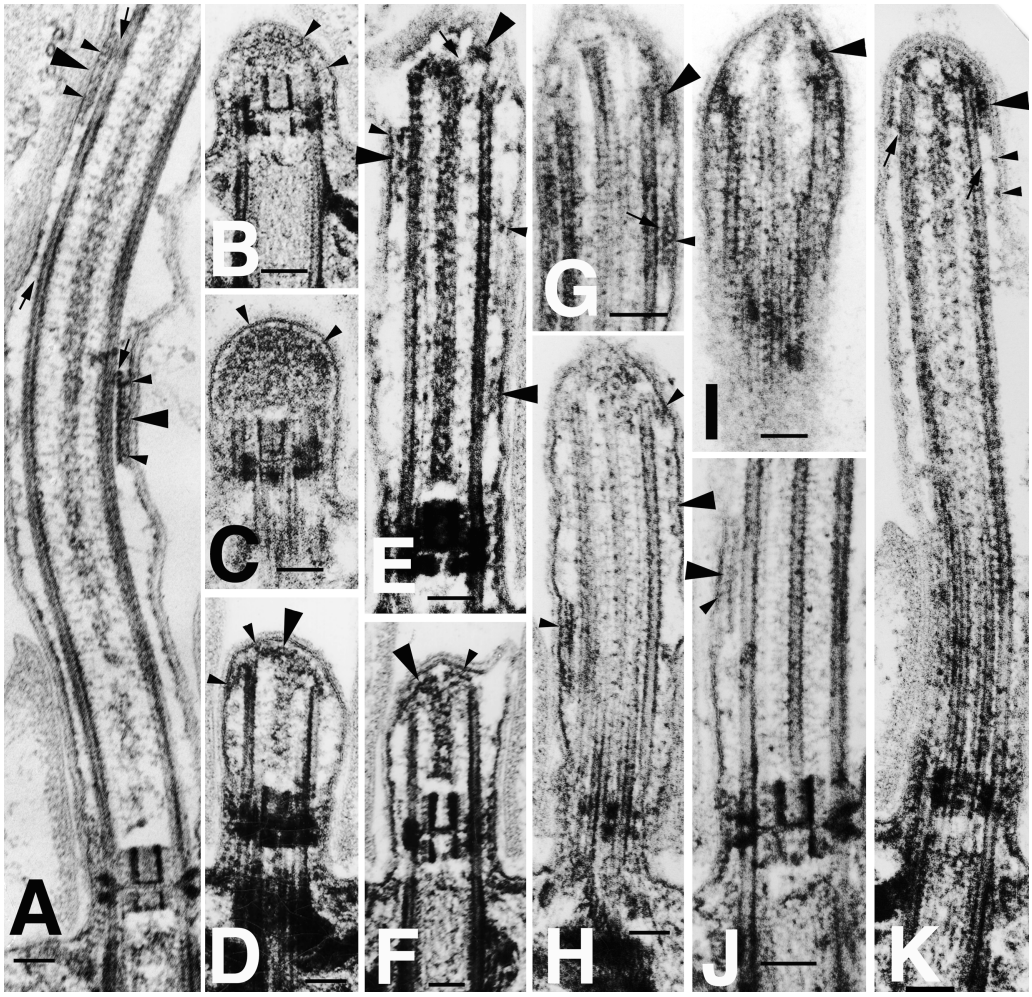


Figure 2. ***pf18* and wild-type *Chlamydomonas* flagella.** Regenerating flagella (B–F) fixed shortly after pH shock-induced deflagellation. IFT particles (arrowheads) are visible in all flagella. In regenerating flagella, numerous particles fill the space distal to the basal body, but by the time microtubules have formed (D), particles have become organized to form linear arrays. IFT particles are linked to the microtubules (small arrows) and to the membrane (small arrowheads). Bars, 0.1 μm.

particle tracks averaged 0.12 ± 0.03 μm (333 tracks) and retrograde tracks averaged 0.06 ± 0.02 μm (326 tracks). There were no significant differences in the sizes of anterograde and retrograde particles in nongrowing flagellar or in flagella induced to shorten with 20 mM sodium pyrophosphate or with high salt, and in flagella regenerating after deflagellation by pH shock. Minor variations in anterograde and retrograde IFT track width (Fig. 1 B) may represent differences in particle size, packing density, or overlapping particles moving along different microtubules, each of which would alter the apparent size in differential interference contrast (DIC) images.

To determine the structure of IFT particles, flagella were examined by EM (see Figs. 1–4). Thin sections of nongrowing flagella (Fig. 1, D–F; Fig. 2, A and G–J; Fig. 3, A and D) revealed the presence of structures similar to the IFT particles identified by Kozminski et al. (1993). Particles appeared either as densely packed structures or as less dense linear particle arrays. IFT particles also were linked to the membrane, most evidently shown when the membrane ballooned away from the axoneme (Fig. 2 A, arrowhead). These membrane links also were visible in newly forming cilia (Fig. 2, B–D) and at the distal microtubule tips of growing or fully-grown flagella (Fig. 2, E–I, K). The particles averaged 0.15 μm in length but could be grouped into two broad classes of large particles, 0.13–0.25 μm, and smaller particles, 0.01–0.09 μm, each of which were comparable to the large (0.12 μm) and small (0.06 μm) particles estimated from kymograph tracks.

To determine when the IFT particles first appear in flagella, *pf18* cells were amputated by pH shock and were fixed and flagella regrew. Early stages of flagellar growth are shown in Fig. 2 (B–E). Flagellar tips were first filled with particles (Fig. 2, B and E), but as microtubules formed, the amorphous particles disappeared and short IFT-like particle aggregates, similar to the moving IFT particles observed by DIC, appeared (Fig. 2, D–H).

In a previous study, a *Chlamydomonas* ulf mutant with bulged flagellar tips full of IFT particles was found to contain numerous small particles linked by filamentous structures (Tam et al., 2003). To determine if the IFT particles seen here have similar structures, flagellated cells were attached to grids,

Published August 15, 2005

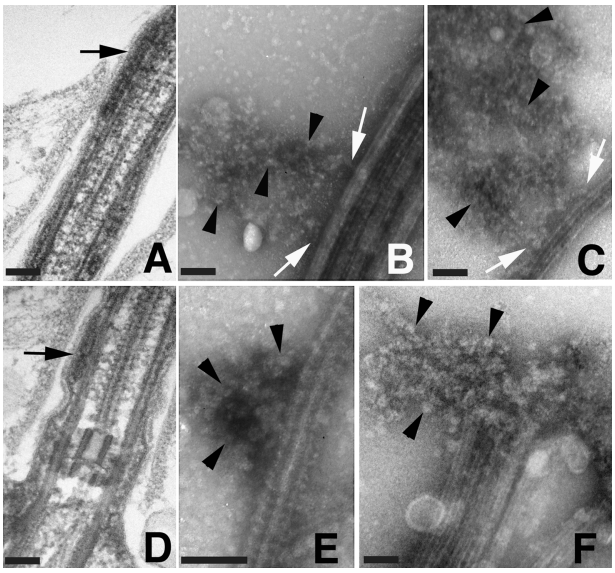


Figure 3. **The structure of IFT particles.** Thin sections (A and D) showing two different-sized IFT particle aggregates (arrows) and negatively stained flagellar whole mounts showing IFT particles (arrowheads) along the sides (B,C, and E) and tips (F) of flagellar microtubules. IFT particles appear to be composed of small strings of smaller particles (B and C) that are linked to the microtubules by short linear structures (white arrows). Strings of IFT particles at the tips of doublets are also shown in E–G. Bars, 0.1 μm.

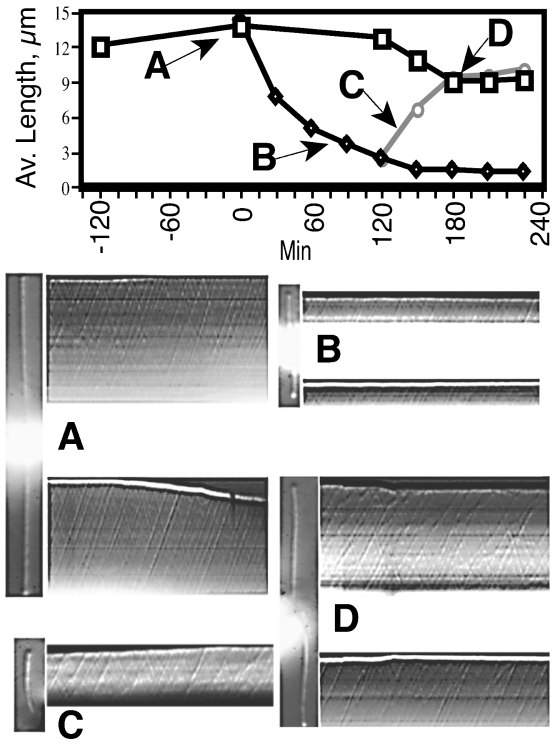


Figure 4. **IFT particle tracks during flagellar shortening and growth.** Addition of 20 mM sodium pyrophosphate to *lf3-2* cells induced rapid shortening of flagella; upon removal of pyrophosphate, flagella rapidly grew to the lengths of control cells (graph). IFT continued in shortening (A and B) and growing (C and D) flagella. In this experiment, the length of flagella on control cells shortened and the growing flagella regenerated to the length of the control cells, even though they were shortening (see Tuxhorn et al., 1998).

extracted with detergent, and negatively stained. As shown in Fig. 3, filamentous particle arrays were found along the sides of microtubules (Fig. 3, B, C, and E) and at the distal microtubule tips (Fig. 3 F). Occasionally these particles formed tight aggregates (Fig. 3 E), but they often spread on the grid to reveal linear particle arrays (Fig. 3, B and C) linked to microtubules by discrete structures, possibly motor proteins.

Because these preparations were made by attaching flagellated cells to grids and extracting them with detergent, it was possible that the particle arrays were unrelated debris caused by the extraction technique. Because IFT particles are depleted in the temperature-sensitive *fla10-1* cells incubated at 32°C (Kozminski et al., 1995), *fla10-1* cells were extracted before and after treatment at 32°C for 60 min. As expected, the filamentous particle arrays were observed in *fla10-1* at room temperature, but only rarely were observed at 31°C. Because occasional IFT particles are seen in *fla10-1* cells examined by DIC microscopy after 1 h at 60°C (unpublished data), these results confirm that the filamentous particle arrays are IFT particles.

### IFT rates and particle frequency in growing and fully grown flagella

The length control hypothesis proposed by Marshall et al. (2005) is based on immunochemical evidence that each flagellum, regardless of its length, contains a fixed number of IFT particles. Because the number of IFT particles/flagellum is fixed, then either the rate of IFT particle movement or the spacing of IFT particles along a flagellum should change as flagella grow or shorten.

To test this hypothesis, the rates of IFT particle movement and the frequency of IFT particles along a flagellum were measured from kymograms similar to those shown in Fig. 1. Rates and particle frequency were measured in nongrowing flagella and in flagella induced to shorten or grow. IFT was recorded in two paralyzed mutants, three mutants with mutations that produce abnormally long flagella, and one mutant with unequal length flagella. Greater than 23,000 individual IFT tracks were measured in 316 different flagella.

As shown in Table I, IFT rates in nongrowing flagella on different flagellar mutants varied slightly, with anterograde rates ranging from 1.6 to 1.9 μm/s and retrograde rates ranging from 2.1 to 2.8 μm/s. There were 1.2–1.4 anterograde and 1.3–1.5 retrograde particle tracks/s. The range of IFT rates and number of particle tracks within any single mutant showed less variation than was observed among different mutants. Colchicine, which blocks microtubule assembly but not the exchange of nontubulin flagellar proteins (Song and Dentler, 2001), had no effect on the IFT rate or frequency.

To determine if IFT rates or particle track frequencies are related to flagellar length, flagellar shortening was induced with 20 mM sodium pyrophosphate (Fig. 4) or by raising the sodium and lowering the calcium concentrations. These were chosen because they are reversible and because they partially paralyze flagella, which makes IFT easy to record. IFT also was recorded when flagella were induced to grow by removal of pyrophosphate (Fig. 4). IFT in growing flagella was observed (a) when cells were washed out of pyrophosphate; (b) in cells assembling new flagella after flagellar

Published August 15, 2005

Table I. **Rate and frequency of anterograde and retrograde particle tracks**

| Cell | | Anterograde rate | Retrograde rate | Ratio A:R rates | Average # anterograde (# counted) | Average # retrograde (# counted) | Ratio A:R | Number of flagella scored |
|---|---|---|---|---|---|---|---|---|
| | | *μm/s* | *μm/s* | | *Tracks/s* | *Tracks/s* | *Tracks/s* | |
| *lf3-2* (*13c2*) | Control | 1.9 ± 0.04 | 2.8 ± 0.04 | 0.68 | 1.4 (2104) | 1.5 (2185) | 0.93 | 37 |
| | 20 mM Na PPi | 2.1 ± 0.04 | 2.6 ± 0.06 | 0.81 | 1.6 (583) | 1.6 (581) | 1.0 | 16 |
| | PPi washout | 2.2 ± 0.04 | 3.5 ± 0.03 | 0.63 | 1.8 (557) | 1.8 (558) | 1.0 | 16 |
| | 20 mM LiCl | 2.1 ± 0.03 | 3.5 ± 0.05 | 0.60 | 1.3 (403) | 1.5 (563) | 0.87 | 10 |
| | Colchicine | 1.9 ± 0.04 | 2.8 ± 0.06 | 0.68 | 1.5 (506) | 1.5 (521) | 1.0 | 13 |
| *pf18* | Control | 1.6 ± 0.04 | 2.5 ± 0.04 | 0.64 | 1.2 (722) | 1.4 (818) | 0.86 | 27 |
| | 20 mM Na PPi | 1.8 ± 0.03 | 2.4 ± 0.04 | 0.75 | 1.2 (585) | 1.5 (705) | 0.80 | 13 |
| | 20 mM LiCl | 1.9 ± 0.02 | 2.8 ± 0.03 | 0.68 | 1.5 (731) | 1.7 (807) | 0.88 | 12 |
| | Hi $Na^+$ low $Ca^{2+}$ | 1.6 ± 0.04 | 2.0 ± 0.06 | 0.80 | 1.2 (407) | 1.0 (476) | 1.2 | 24 |
| *pf16* (*13a2*) | Control | 1.6 ± 0.04 | 2.6 ± 0.04 | 0.62 | 1.2 (1144) | 1.7 (1495) | 0.71 | 61 |
| | 20 mM Na PPi | 2.0 ± 0.04 | 2.6 ± 0.04 | 0.77 | 1.7 (1571) | 1.8 (1675) | 0.94 | 27 |
| | PPi washout | 1.7 ± 0.03 | 2.5 ± 0.04 | 0.68 | 1.4 (447) | 1.7 (527) | 0.82 | 8 |
| *lf2* | Control | 1.8 ± 0.04 | 2.1 ± 0.06 | 0.86 | 0.9 (685) | 1.3 (829) | 0.69 | 22 |
| *lf4* | 20 mM Na PPi | 1.9 ± 0.04 | 2.6 ± 0.6 | 0.73 | 1.3 (402) | 1.5 (486) | 0.87 | 8 |
| *ulf2* | Control | 1.5 | 2.9 | 0.52 | 1.2 (402) | 1.4 (486) | 0.86 | 9 |
| Average for all flagella | | 1.9 | 2.7 | 0.70 | 1.4 (11,249) | 1.5 (12,712) | 0.93 | 316 |

Anterograde and retrograde frequencies of IFT in flagella on control cells and cells treated with sodium pyrophosphate, colchicine, LiCl, or high $Na^+$ low $Ca^{2+}$.

amputation induced by pH shock (see Fig. 6, see Table IV); and (c) in cells flagella induced to elongate by 20 mM LiCl (Tuxhorn et al., 1998).

In five different *Chlamydomonas* mutants, the rate and number of anterograde and retrograde particle tracks over a 40-s (600 image) time period exhibited little variation rela-

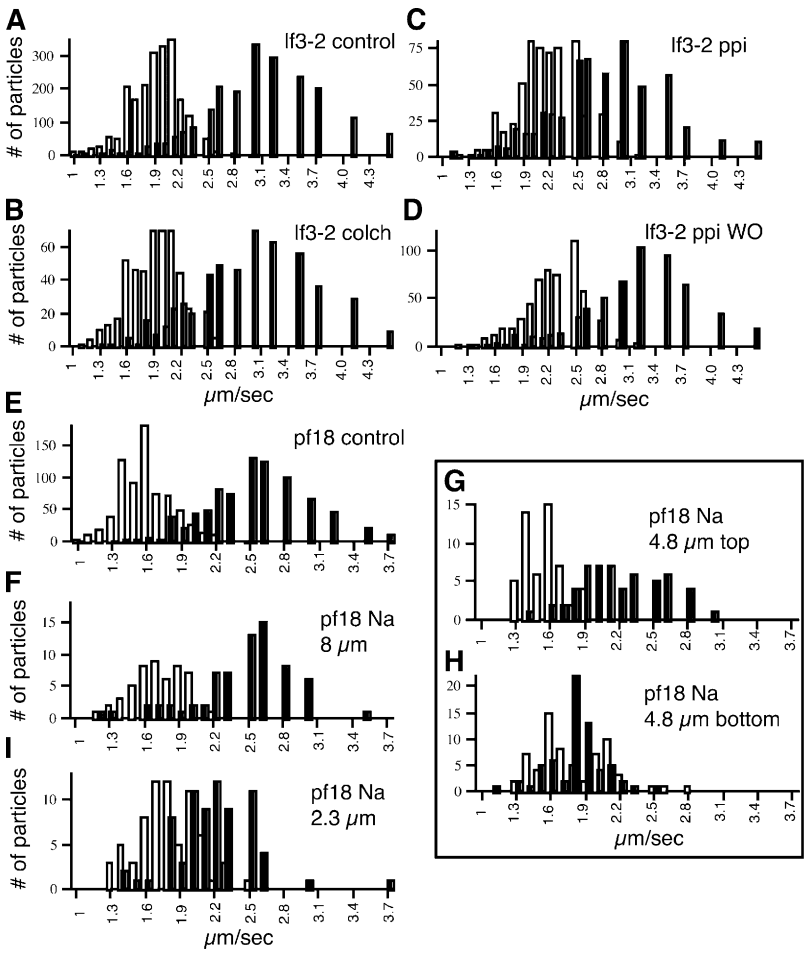


Figure 5. **Histogram showing representative data from Table I.** The rate of IFT particle movement (μm/s) is plotted on the X-axis and the number of measurements is plotted on the Y-axis. A–D show *lf3-2* and E–I show *pf18* flagellar measurements. Anterograde (base to tip) (open bars) and retrograde (filled bars) rates are shown for each mutant and treatment. Control (A) and colchicine-treated *lf3-2* (B) and *pf18* control (E) flagella show typical distributions of anterograde and retrograde transport. Similar distributions are found in averaged populations of flagella treated with 20 mM pyrophosphate (C and D). Sort flagella induced by low $Ca^{2+}$ and high NaCl revealed that flagella shorter than 4–5 μm have reduced retrograde IFT rates (H and I). G and H show IFT rates in two flagella on the same cell, one of which shows nearly identical anterograde and retrograde IFT rates and the other shows significantly faster retrograde IFT.

Published August 15, 2005

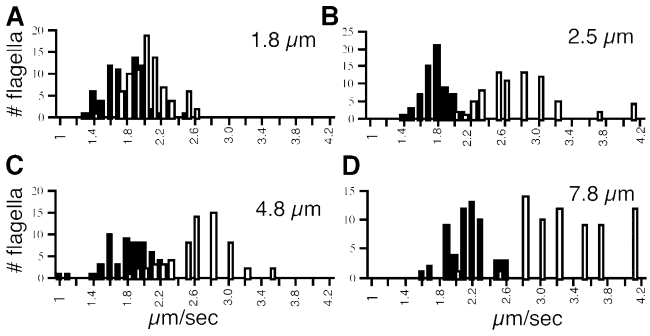


Figure 6. ***pf18* cells were deflagellated and IFT was recorded as flagella regenerated.** Average rates of anterograde and retrograde IFT are presented in Table IV and the distribution of IFT particle rates within individual flagella are shown in the histograms. In short flagella the differences between anterograde and retrograde IFT rates were significantly less than with 2.5 μm or longer flagella.

tive to flagellar length (Table I). Histograms of the rates of representative flagella, which provide a better indication in the variation and distribution of rates, are shown in Fig. 5, and histograms of flagella regenerating after pH shock are shown in Fig. 6.

Although the average IFT rates did not significantly change as flagella shortened and grew, some shifts in IFT rates did occur in very short flagella. Cells induced to shorten flagella with high salt (Lefebvre et al., 1978) exhibited frequencies of IFT similar to those in control cells (Fig. 5, compare A, B, and E with F) until flagella were shorter than ~4 μm., at which length retrograde IFT rates decreased (Fig. 5, compare F and I). In 4–5-μm-long flagella, two flagella on the same cell exhibited different distributions of rates of retrograde and anterograde IFT during the 40-s recording period (Fig. 5, G and H). A slight increase in the distribution of anterograde IFT was observed during rapid flagellar growth after cells were transferred from pyrophosphate, but this returned to control rates as the flagella elongated (Fig. 5, compare C and D with A and B). Short regenerating flagella after pH shock also showed similar anterograde and retrograde IFT rates, but as flagella grew longer than 4 μm, the distribution of anterograde and retrograde rates reached those of control flagella (Fig. 6, Table IV).

Together, these data reveal that IFT rates and frequency, averaged over a 40-s period, are nearly constant in five different flagellar mutants, and that the rates and frequency of IFT are nearly constant in nongrowing, shortening, and growing flagella. Flagella shorter than 4 μm exhibit a slightly slower rate of retrograde IFT than do flagella longer than 4 μm, which may indicate important differences between short and longer flagella.

## IFT particle accumulations do not impede IFT

Most IFT particles move completely to the distal flagellar tip, by kinesin-2, and then are transported proximally to the flagellar base by cytoplasmic dynein (Pazour et al., 1998; Porter et al., 1999). Switches that regulate motor activity are likely to be located at the distal flagellar tip. Two classes of *Chlamydomonas* mutants accumulate particles at flagellar tips. The tips cDhc1b flagellar mutants fill with IFT particles and disassemble. Observations of these flagella suggested that IFT particle accumulations might stimulate flagellar disassembly. By contrast, IFT particles fill the tips of unequal length (ulf) flagellar mutants, but these flagella grow more than twice the length of normal flagella, despite the accumulation of IFT particles at their tips (Tam et al., 2003). Because flagellar growth in ulf mutants is slower than that in wild-type cells, it is possible that IFT particle accumulations at the tips may alter IFT rates or alters the switches that induce retrograde transport (Tam et al., 2003; unpublished data).

Surprisingly, both the rates and frequencies of IFT in *ulf-2* flagella were similar to those for other cells (Fig. 7, Table I).

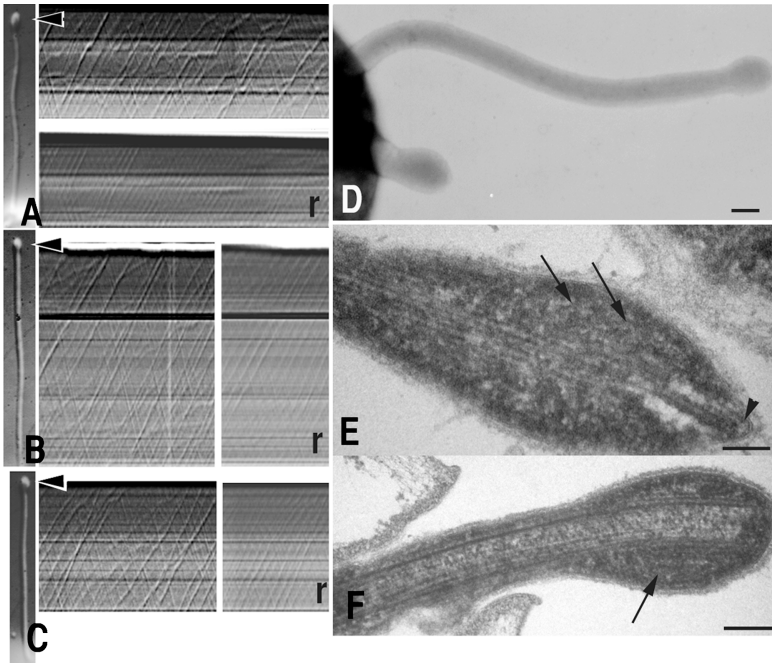


Figure 7. **Unequal length flagellar mutants showing bulbous tips filled with IFT particles.** The tips of these flagella are bulbous (A–C, arrowheads) and are filled with IFT material, some of which can be seen as linear arrays (E and F, arrows). Capping structures also are present at microtubule tips (E, arrowhead). Kymographs to the right of A–C show normal anterograde and retrograde IFT. Linear reinforcements of the kymographs (r) reveal the maximum IFT periodicity (see the "IFT particle entry into flagella is periodic" section). Bars, 0.1 μm.

Published August 15, 2005

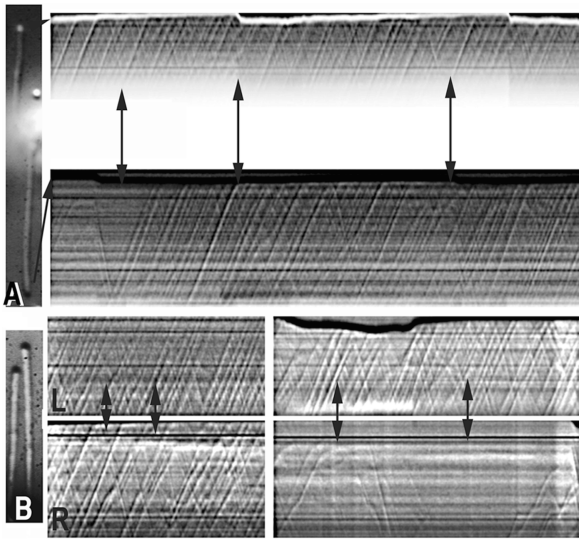


Figure 8. **IFT starts and stops (*pf16*).** Pairs of flagella on the same cell were recorded and kymographs generated. Double arrowheads point to differences in tracks in the two flagella as well as pauses that occur in one but not the other flagellum.

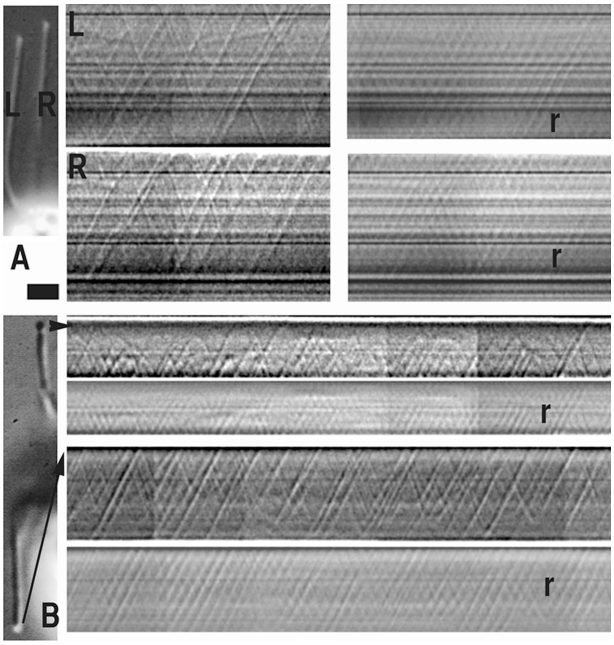


Figure 9. **Periodicity of entry of IFT particles into the flagellum.** (A) *lf2* flagellar tracks were longitudinally reinforced to reveal periodic anterograde and retrograde IFT. Both flagella on this cell exhibited the same periodicity even though they did not show simultaneous patterns of IFT within the two flagella. IFT movements in both flagella were recorded simultaneously. (B) (*pf18*) flagella show exhibit the same periodicity of IFT transport even though patterns of individual tracks were not simultaneous. Tracks in the bottom flagellum were inverted (the arrows point to the flagellar tips). Reinforced images (r) are shown below the 40-s (600 image) films.

Anterograde IFT in *ulf-2* flagella was slightly slower than that measured in other flagella (Table I), as was the periodicity of IFT particles (see Table III), which suggests that the accumulation of IFT particles at the tips may slow flagellar assembly and have small effects on IFT rate and frequency; but these effects are small, relative to the rates and frequencies observed in flagella that lack such particle accumulations.

### IFT particle entry into flagella is periodic

In *Chlamydomonas*, two flagella usually grow at the same time and are nearly equal in length, which suggests that IFT in the two flagella may be coordinated. Alternatively, the observations of ulf mutants, with unequal length flagella, the independent flagellar shortening and growth on cells with one amputated flagellum (Rosenbaum et al., 1969) and the selective shortening of long flagella on mated lf and wild-type cells (Asleson and Lefebvre, 1998) suggested that IFT in the two flagella may not be coordinated. To determine if IFT is coordinated in two flagella, IFT was recorded in both flagella on individual cells was recorded for most of the cells described here. Representative IFT tracks in both flagella are shown in Fig. 8 (also see Fig. 4 A, B, and D; Fig. 9).

Comparison of the two flagella revealed that anterograde and retrograde tracks were not uniformly spaced, and occasionally pauses of several seconds occurred during which no IFT was observed in one flagellum while IFT proceeded normally in the sister flagellum (Fig. 8). No anterograde or retrograde IFT was observed during these pauses, which indicates that no IFT particles entered the flagellum during the pauses. These data show that IFT is not well coordinated between the two flagella on a single cell.

The periodicity of particle entry was examined by longitudinal reinforcement of IFT track images (Dentler and Cunningham, 1977; Kim et al., 1979). These images (Fig. 4; Fig. 7, A–C) revealed that particle entry into a flagellum is periodic and that, even after a pause in particle entry into the flagellum (no IFT tracks found in the flagellum), particle entry resumed in accordance with the period of other tracks. Additionally, both anterograde and retrograde periodicities were enhanced, indicating that they are coordinated. As with the anterograde and retrograde rates, the period of particle entry did not significantly change during flagellar growth or resorption and was consistent in all cells examined. For the 199 flagella examined, the average number of starts/s was 4.2 ± 0.6 (Table II). This was greater than the average number of IFT tracks/flagellum observed for 40 s (Table I), which is consistent with periodic pauses observed in the entry of particle tracks into flagella seen in kymographs presented here.

### The number of IFT particles is not fixed, but is a function of flagellar length

The number and frequency of particle tracks do not appear to be related to flagellar growth, so the number of particles within a flagellum should be proportional to flagellar length. To confirm this, the number of particle tracks within a 1- or 2-μm × 1 min area was counted. The results (Table III) show that growing, shortening, and control flagella contain an average of 3.8 ± 0.7 particles/μm/s. The same particle number was found in short (<4 μm) and long flagella and at randomly chosen positions within flagella. The number of particles per flagellum was determined by multiplying the number of particles by flagellar length and varied between 12 and 50, depending on the flagellar length. Thus, the number of flagellar IFT particles is not fixed, but rather, is a function of flagellar length.

Published August 15, 2005

Table II. **Average periodicity of IFT tracks**

| Cell | Treatment | Period (# starts/s) | Number of reinforced flagella |
|---|---|---|---|
| | Control | 4.3 ± 0.6 | 31 |
| | Colchicine | 4.1 ± 0.7 | 12 |
| *lf3-2* (*13c2*) | LiCl | 4.0 ± 0.0 | 10 |
| | 20 mM Na PPi | 4.1 ± 0.4 | 9 |
| | ppi WO | 4.4 ± 0.7 | 16 |
| *pf16* (*13a2*) | Control | 3.9 ± 0.8 | 24 |
| | 20 mM Na PPi | 4.1 ± 0.3 | 23 |
| | ppi WO | 4.3 ± 0.6 | 8 |
| | LiCl | 5.0 ± 0.4 | 4 |
| *pf18* | Control | 3.9 ± 0.6 | 12 |
| | LiCl | 4.5 ± 0.6 | 11 |
| | 20 mM Na PPi | 4.5 ± 0.7 | 11 |
| *lf2* | Control | 4.3 ± 0.6 | 12 |
| *lf3* | Control | 3.8 ± 0.8 | 9 |
| *ulf2* | Control | 3.7 ± 0.6 | 7 |
| AV | | 4 ± 0.3 | 199 |

IFT track images were duplicated in Photoshop layers, and layers were shifted to reveal periodicity. Numerous spacings were tested and a minimum of four shifts was used to identify periodicity. Periodicity was only obtained on individual images at the spacings indicated.

Table III. **Average number of IFT particles/μm/s**

| Cell | Treatment | Number of flagella counted | Average IFT particles/μm (# particles counted) |
|---|---|---|---|
| | Control | 10 | 4 (86) |
| | LiCl | 12 | 3 (90) |
| *lf3-2* (*13c2*) | 20 mM Na PPi | 8 | 4 (66) |
| | Na PPi | 6 | 5 (60) |
| | Na PPi wash-out | 17 | 4 (115) |
| *pf16* (*13a2*) | Control | 12 | 3 (103) |
| | LiCl | 4 | 3 (39) |
| | 20 mM Na PPi | 16 | 4 (66) |
| *ulf2* | Control | 4 | 4 (33) |
| Average | | | 3.8 ± 0.7 |

Average number of IFT particles/μm/s. A box, 1 or 2 μm × 1 s, was scanned across kymographs of 72 different flagella and the number of tracks were counted to obtain the number of IFT particles present in the 1- or 2-μm box during a 1-s period of time.

## Discussion

The mechanisms that regulate the lengths of eukaryotic cilia and flagella remain a mystery. Their assembly and disassembly have been well documented, as have numerous mutants with abnormally short or abnormally long flagella and cells that contain cilia with different lengths (Dentler, 1981, 1987; Lefebvre and Rosenbaum, 1986). Even within individual flagella, the regulation of microtubule length must be locally controlled. In ctenophore macrocilia, many individual axonemes are contained in a single membrane and each axoneme has its own characteristic growth rate and final length (Tamm and Tamm, 1988). Within single axonemes, there is clear evidence for independent regulation of the lengths of specific doublet microtubules (Tyler, 1979) and central microtubules (Omoto and Witman, 1981). Although mechanisms that regulate assembly are unknown, it is clear that flagellar microtubules and associated structures assemble at the distal tips (Johnson and Rosenbaum, 1992), so one site of length regulation is likely associated with these tips, possibly with microtubule capping structures (Dentler, 1980; Dentler and Rosenbaum, 1977).

Flagellar components appear to be transported to the distal tips by IFT (Kozminski et al., 1995; Cole et al., 1998; Piperno et al., 1998; Pazour and Rosenbaum, 2002; Rosenbaum and Witman, 2002; Qin et al., 2004; Snell et al., 2004). Flagellar assembly requires both kinesin-2 (Walther et al., 1994; Matsuura et al., 2002; Mueller et al., 2005) and cytoplasmic dynein (Pazour et al., 1998, 1999; Porter et al., 1999). In the temperature-sensitive kinesin-2 *Chlamydomonas* mutant *fla10-1*, both IFT and flagellar protein incorporation ceases at 32°C, and IFT (Song and Dentler, 2001; Kozminski et al., 1995; Piperno et al., 1998) and flagella disassemble, which confirms that IFT is required for assembly. The role of IFT in flagellar disassembly is less certain. At restrictive temperature, *fla10-1* flagella shorten without IFT (Kozminski et al., 1995; Iomini et al., 2001), so IFT may only be necessary to return anterograde motors and



Table IV. **IFT during flagellar regeneration**

| Length | Anterograde rate | Retrograde rate | Ratio A:R rate | Number anterograde | Number retrograde | Ratio A:R track number |
|---|---|---|---|---|---|---|
| *μm* | *μm/s* | *μm/s* | | *Tracks/s* | *Tracks/s* | |
| 1.5 | 1.6 ± 0.04 | 2.0 ± 0.04 | 0.8 | 75 | 87 | 0.9 |
| 1.5 | 1.6 ± 0.03 | 2.1 ± 0.04 | 0.8 | 74 | 72 | 1.0 |
| 1.8 | 1.8 ± 0.03 | 2.1 ± 0.06 | 0.9 | 83 | 76 | 1.1 |
| 1.8 | 1.7 ± 0.04 | 2.0 ± 0.03 | 0.9 | 71 | 80 | 0.9 |
| 2.3 | 1.8 ± 0.03 | 2.1 ± 0.04 | 0.9 | 80 | 80 | 1.0 |
| 2.3 | 1.6 ± 0.03 | 1.9 ± 0.04 | 0.8 | 57 | 67 | 0.9 |
| 2.5 | 1.8 ± 0.03 | 2.6 ± 0.03 | 0.7 | 65 | 76 | 0.9 |
| 3.5 | 1.8 ± 0.03 | 2.5 ± 0.03 | 0.7 | 58 | 72 | 0.8 |
| 4.0 | 1.8 ± 0.04 | 2.6 ± 0.03 | 0.7 | 55 | 64 | 0.9 |
| 4.8 | 2.1 ± 0.03 | 2.8 ± 0.04 | 0.8 | 64 | 62 | 1.0 |
| 5.8 | 1.6 ± 0.04 | 2.5 ± 0.03 | 0.6 | 69 | 75 | 0.9 |
| 6.8 | 2.2 ± 0.03 | 3.8 ± 0.03 | 0.6 | 71 | 73 | 1.0 |
| 7.8 | 1.7 ± 0.03 | 2.8 ± 0.03 | 0.6 | 52 | 53 | 1.0 |

Number and rate of IFT particle tracks during flagellar shortening and growth.

Published August 15, 2005

IFT proteins to the cell body. Flagellar disassembly may occur by IFT-independent removal of flagellar components near the basal body (Stephens, 2000; Parker and Quarmby, 2003).

Based on the importance of IFT, the rate of flagellar assembly, immunoblot analysis of IFT proteins, and the exchange of flagellar proteins with a cytoplasmic pool (Gorovsky et al., 1970; Stephens, 2000; Song and Dentler, 2001), Marshall et al. (2005) proposed a "balance-point equilibrium" hypothesis in which the number of IFT particles in a flagellum is constant, regardless of flagellar length, and that the number and rate of movement of IFT particles determines flagellar length.

If the number of IFT particles in a flagellum is constant, either the frequency of IFT particles along the flagellum must decrease as flagella grow or the rate of anterograde or retrograde particle movement should decrease. Conversely, as flagella shorten, the frequency of particles along flagella should increase or IFT rates must increase. In the data reported here, no significant differences in IFT rate or frequency were observed in steady-state flagella on several different *Chlamydomonas* mutants. The same rates and particle frequencies were observed in flagella induced to shorten by sodium pyrophosphate or high $Na^+$/low $Ca^{2+}$ treatment. When washed back into culture medium or Hepes buffer, flagella regrew but maintained the same IFT rates and frequencies. Similar results were observed in flagella growing after pH shock amputation of old flagella. The data reported here do not support the balance-point hypothesis.

In flagella shorter than ~4 μm there was a slight reduction of the retrograde IFT rate compared with longer flagella, but this was not sufficient to support the balance-point hypothesis. This slight difference may be interesting to examine further, particularly with the discovery of two motors, moving at different rates in the proximal and distal regions of *Caenorhabditis elegans* cilia (Snow et al., 2004).

Examination of individual particle tracks revealed numerous gaps or pauses in IFT particle entry into flagella. Based on the number of anterograde particle tracks observed during the 40-s recordings, particles entered flagella at an average of 1.4 particles/s. When the periodicity of particle entry was examined by longitudinal reinforcement of the kymographs, particle entry appeared to be periodic, with a maximum of 4 particles/s that could enter and leave the flagellum. This indicates that particle entry is periodically regulated and that the pauses or gaps in particle entry may reflect the readiness of a particle to pass a checkpoint. Because the pauses were not coordinated between two flagella on a single cell, IFT particle entry may be regulated individually by each flagellum. The nature of the entry checkpoint is not understood but it might be associated with proteins identified by Deane et al. (2001).

IFT particle accumulations at the tips of ulf mutants (Tam et al., 2003) might be expected to interfere with either the reversal of IFT particle movement or with flagellar growth or disassembly. Flagellar assembly progressed more slowly in these mutants than in wild-type cells (Tam et al., 2003; unpublished data) and the rate of anterograde IFT was slightly reduced from those in wild-type flagella. However, retrograde transport and frequency was not reduced, so the accumulation of IFT particles at flagellar tips seem to present no major obstacle to IFT particle movement or to the switching of motors that start retrograde particle movement.

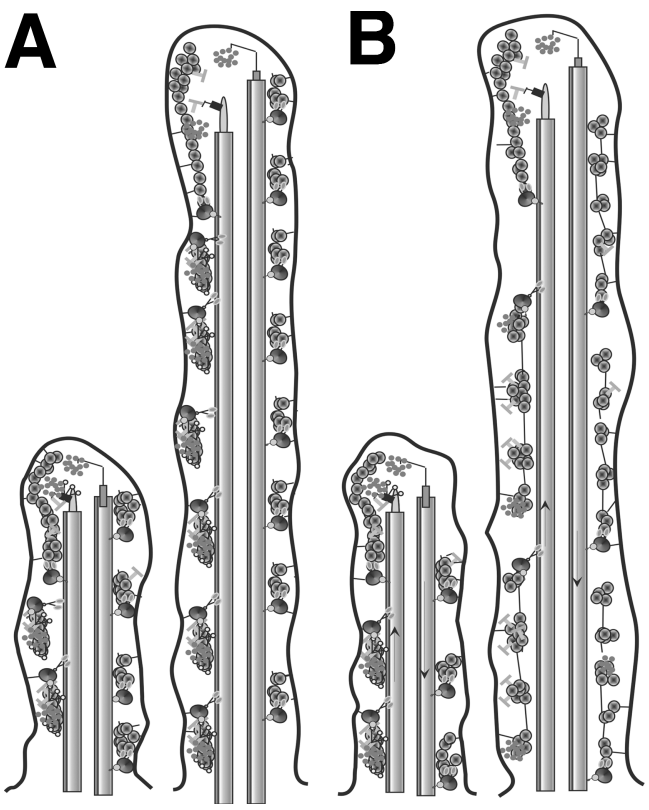


Figure 10. **Interpretation of IFT images.** Two representative flagellar microtubules are drawn. Model A: the number of IFT particles is proportional to flagellar length. Model B: the number of IFT particles/flagellum is constant but the shape of particles change as flagella elongate. Each small clump of particles would appear as a single particle by DIC, so the number of particle tracks would be proportional to flagellar length but the absolute number of particles would remain a constant.

The kymographs also revealed that retrograde particles were approximately half the size of anterograde particles, and similar sized particles were found using electron microscopy. As deflagellated cells regenerate flagella, the particles fill the region distal to the basal body and often appear attached to the membrane and, as flagellar microtubules assemble, small particle aggregates are formed. These aggregates are linked by filamentous structures, best observed in negatively stained flagella. The particles are attached both to the microtubules, presumably by the motor proteins, and to the membrane by short structures. The membrane-attachment of IFT particles has not been described previously but they may be related to the cytoplasmic dynein-containing microtubule–membrane bridges first identified in *Tetrahymena* and scallop cilia (Dentler et al., 1980). Further characterization of IFT particle structure and their associations with flagellar membranes will be important.

Can data presented here, showing that the number of IFT particles is a function of flagellar length, be reconciled with the balance-point hypothesis, in which the number of IFT particles recognized by antibodies in each flagellum appears to be fixed (Marshall and Rosenbaum, 2001; Marshall et al., 2005)? Two

Published August 15, 2005

models are presented in Fig. 10. Model A is consistent with data presented here, in which the number of IFT particles increases with flagellar length. This model predicts that particles in addition to those identified immunologically may remain to be discovered. Model B is based on the structure of IFT particles and indicates that some of the particle aggregates may stretch along the microtubules and produce small densities observed in the kymographs. In this model, the number of IFT particle aggregates in a flagellum would remain constant but the number of visible particles would be proportional to flagellar length. Further studies will be required to identify additional IFT components or to define ways the particle aggregates can form multiple IFT aggregates seen by DIC.

Rather than regulating the number of particles within a flagellum, it is likely that flagellar microtubule length is regulated by the loading of flagellar proteins on IFT particles, at flagellar bases, and the unloading of proteins from IFT particles, at flagellar tips. Three proteins, mutations in which cause abnormally long flagella (LF1, LF2, LF3), form particulate structures in the cell body and may be involved in loading material onto IFT particles (Barsel et al., 1988; Asleson and Lefebvre 1998; Tam et al., 2003; Nguyen et al., 2005), and a fourth protein (LF4) is located in the flagellum (Berman et al., 2003). A *Chlamydomonas* aurora-like kinase (CALK) associated with flagellar disassembly has been identified (Pan et al., 2004), but the location of CALK is not understood. It is likely that these components are associated with signaling systems that determine the length of individual microtubules and, as previously suggested (Dentler, 1981), it is reasonable to suggest that the selection of components for individual microtubules from the IFT transport particles is performed by proteins associated with the capping structures at microtubule tips.

## Materials and methods

*Chlamydomonas* cells were cultured in minimal medium (Sager and Granick, 1953) with continuous aeration on a 12-h light/ dark cycle and were used 3–4 h after the start of the light period. Paralyzed mutants (*pf18* [cc1036)], *lf3-2* [*13c2*, from a cross between *lf3* and *pf16*)], *pf16* [*13a2*, from a cross between *lf3* and *pf16*]) were used to facilitate recording IFT. Motile *lf2* and ulf cells were paralyzed with 20 mM pyrophosphate (pH 7.0) or 20 mM LiCl. LF, *13c2*, *13a2*, and ulf mutants were obtained from L.-W. Tam and P. Lefebvre (University of Minnesota, St. Paul, MN), and *pf18* from the *Chlamydomonas* Genetics Center.

### Light microscopy and analytical methods

For microscopy, #0 (22 × 22 mm) and #1 (24 × 60 mm) coverslips (Gold Seal #3026 and #3323, respectively) were cleaned in deionized water and detergent, rinsed in deionized water, and oven dried. Cleaned 24 × 60-mm coverslips were attached with double-stick tape to 25 × 75 × 1-mm aluminum bars prepared with a 22 × 22-mm cutout. Cleaned 22 × 22 mm coverslips were treated with 1 mg/ml poly-L-lysine for 2–12 h and rinsed with deionized water and culture medium or HM (50 mm Hepes, pH 7.1, and 2 mM $MgSO_4$) immediately before applying cells.

Cells were pelleted in a clinical centrifuge and gently suspended in fresh minimal medium or in HMC (HM + 1 mM $CaCl_2$). 4-ml aliquots of cells were placed in 6-well culture dishes and rotated at RT for the duration. For length measurements, 100-μl aliquots of cells were fixed with 100 μl of 2% glutaraldehyde in HMC.

To prepare IFT chambers, 50 μl of the suspended cells were applied to poly-lysine–treated coverslips, incubated for 1–3 min, and then inverted over the mounted 24 × 60-mm coverslip. The two coverslips were separated by Parafilm strips. Excess medium was removed with filter paper and chambers were sealed with VALAP (1:1:1 Vaseline/Lanolin/Paraffin).

Cells were viewed at RT with a microscope (Axioplan 2ie; Carl Zeiss MicroImaging, Inc.), 100×/1.4 PlanApochromat lens, 1.4 NA condenser lens, and DIC optics. Samples were illuminated using a 100-W halogen lamp, UV and green interference filters. Cells were healthy for at least 3 h of recording. Images were projected onto a Nuvicon camera (Dage-MTI) using a 1.6× optovar (Carl Zeiss MicroImaging, Inc.) and an 8× eyepiece in a projection tube (Carl Zeiss MicroImaging, Inc.), and contrast was enhanced using Dage and Image Σ image processors. Images were collected at 15 frames/s for 600 frames (40 s) with a Macintosh 6500 computer, and Scion frame grabber board.

Cells were selected for the presence of straight flagella and the orientation of their flagella relative to the DIC shear. Whenever possible, cells in which IFT could be observed in both flagella were selected. Image stacks were transferred to a Macintosh G4 computer and opened in Image J (http://rsb.info.nih.gov/ij/). To produce kymographs, images were rotated to orient each flagellum vertically, with the flagellar distal tip at the top. A selection containing part or all of the flagellum was made, resliced, and Z-projected on screen. IFT rates were determined by measuring the angle of the IFT particle tracks using Image J and measurements were recorded and transferred to Excel (Microsoft). Kymographs, saved as TIFF files, were filtered using Photoshop CS (Adobe Corp.) by applying Gaussian blur (0.7) and unsharp mask (298%, 2.7 pixel radius, 1 threshold). For optical reinforcements, filtered kymographs were selected, copied to new layers, reduced to 30% transparency, and moved to generate reinforcements. The distance shifted was measured using Photoshop.

### Flagellar elongation and shortening

To induce flagellar shortening, cells were harvested and suspended in minimal medium with 20 mM sodium pyrophosphate (pH 7.0) (Lefebvre et al., 1978). This also paralyzed flagella, which facilitated IFT recordings. Flagellar regrowth was observed by harvesting cells from pyrophosphate and suspending them in fresh medium. Flagellar resorption also was induced by suspending cells medium containing low $Ca^{2+}$, 25 mM NaCl, and 0.7 mM KCl (Lefebvre et al., 1978). To observe newly assembling flagella, cells were amputated by pH shock and allowed to regenerate (Lefebvre, 1995). Flagellar length in the population of cells were determined by fixing cells with an equal volume of medium containing 2.5% glutaraldehyde and measuring lengths using Image J.

### Electron microscopy

For thin sections, cells were cultured as described above, gently pelleted, suspended in M medium, and were fixed by adding an equal volume of M medium containing 5% glutaraldehyde and embedding in Embed 812 (Dentler and Adams, 1992). Sections were stained with methanolic uranyl acetate followed by lead citrate.

A modification of the method described by Dentler and Rosenbaum (1977) was used for negative staining. Cells were concentrated and suspended in a small volume of HMC (10 mM Hepes, 0.1 mM $CaCl_2$, and 1 mM $MgSO_4$) and a drop of cells was applied to a poly-λ-lysine treated carbon-formvar film on a copper grid. The grid, containing cells, was then inverted over a drop of HMC at 4°C followed by inversion over 0.005–0.1% Nonidet P-40 detergent in HMC for 5–20 s at 4°C. Cells then were rinsed with cold HMC, stained, with 1% aqueous uranyl acetate, and air dried. Samples were examined with a transmission electron microscope (1200 EXII; JEOL), photographed using a MegaView camera (Soft Imaging System); images were adjusted for contrast and cropped using Photoshop.

I thank Dr. David Moore-Nichols for help with Image J, Dr. Pete Lefebvre for supplying cell stocks and for critical reading of this manuscript, Drs. Sid Tamm and Lai-Wa Tam for many helpful comments, and Dr. Bill Snell for his encouragement.

Submitted: 3 December 2004
Accepted: 13 July 2005

## References

Asleson, C.M., and P.A. Lefebvre. 1998. Genetic analysis of flagellar length control in *Chlamydomonas reinhardtii*: a new long-flagella locus and extragenic suppressor mutations. *Genetics*. 148:693–702.

Barsel, S.-E., D.E. Wexler, and P.A. Lefebvre. 1988. Genetic analysis of long-flagella mutants of *Chlamydomonas reinhardtii*. *Genetics*. 118:637–648.

Berman, S.A., N.F. Wilson, N.A. Haas, and P.A. Lefebvre. 2003. A novel MAP kinase regulates flagellar length in *Chlamydomonas*. *Curr. Biol.* 13:1145–1149.

Bloodgood, R.A. 1977. Motility occurring in association with the surface of the *Chlamydomonas* flagellum. *J. Cell Biol.* 75:983–989.

Cole, D.G. 2003. The intraflagellar transport machinery of *Chlamydomonas reinhardtii*. *Traffic*. 4:435–442.

Cole, D.G., D.R. Diener, A.L. Himelblau, P.L. Beech, J.C. Fuster, and J.L. Rosenbaum. 1998. *Chlamydomonas* kinesin-II-dependent intraflagellar transport (IFT): IFT particles contain proteins required for ciliary assembly in *Caenorhabditis elegans* sensory neurons. *J. Cell Biol.* 141:993–1008.

Deane, J.A., D.G. Cole, E.S. Seely, D.F. Diener, and J.L. Rosenbaum. 2001. Localization of the intraflagellar transport protein IFT52 identifies the transitional fibers of the basal bodies as the docking site for IFT particles. *Curr. Biol.* 11:1586–1590.

Dentler, W.L. 1980. Structures linking the tips of ciliary and flagellar microtubules to the membrane. *J. Cell Sci.* 42:207–220.

Dentler, W.L. 1981. Microtubule-membrane interactions in cilia and flagella. *Int. Rev. Cytol.* 72:1–47.

Dentler, W.L. 1987. Cilia and flagella. *Int. Rev. Cytol. Suppl.* 17:391–456.

Dentler, W.L. 1990. Linkages between microtubules and membranes in cilia and flagella. *In* Ciliary and Flagellar Membranes. R.A. Bloodgood, editor. Plenum Publishing, New York. 31–64.

Dentler, W.L., and C. Adams. 1992. Flagellar microtubule dynamics in *Chlamydomonas*: cytochalasin D induces periods of microtubule shortening and elongation; colchicine induces disassembly of the distal, but not proximal, half of the flagellum. *J. Cell Biol.* 117:1289–1298.

Dentler, W.L., and W.P. Cunningham. 1977. Structure and organization of radial spokes in cilia of *Tetrahymena pyriformis*. *J. Morphol.* 153:143–151.

Dentler, W.L., and J.L. Rosenbaum. 1977. Flagellar elongation and shortening in *Chlamydomonas* III. Structures attached to the tips of flagellar microtubules and their relationship to the directionality of microtubule assembly. *J. Cell Biol.* 74:747–759.

Dentler, W.L., M.M. Pratt, and R.E. Stephens. 1980. Microtubule-membrane interactions in cilia. II. Photochemical cross-linking of bridge structures and the identification of a membrane-associated ATPase. *J. Cell Biol.* 84:381–403.

Gorovsky, M.A., K. Carlson, and J.L. Rosenbaum. 1970. Simple method for quantitative densitometry of polyacrylamide gels using fast green. *Anal. Biochem.* 35:359–370.

Iomini, C., V. Babaev-Khaimov, M. Sassaroli, and G. Piperno. 2001. Protein particles in *Chlamydomonas* flagella undergo a transport cycle consisting of four phases. *J. Cell Biol.* 153:13–24.

Iomini, C. K. Tejada, W. Mo, H. Vaananen, and G. Piperno. 2004. Primary cilia of human endothelial cells disassemble under laminar shear stress. *J. Cell Biol.* 164:811–817.

Johnson, K.A., and J.L. Rosenbaum. 1992. Polarity of flagellar assembly in *Chlamydomonas*. *J. Cell Biol.* 119:1605–1611.

Kim, H., L.I. Binder, and J.L. Rosenbaum. 1979. The periodic association of MAP2 with brain microtubules *in vitro*. *J. Cell Biol.* 80:266–276.

Kozminski, K.G., K.A. Johnson, P. Forscher, and J.L. Rosenbaum. 1993. A motility in the eukaryotic flagellum unrelated to flagellar beating. *Proc. Natl. Acad. Sci. USA*. 90:5519–5523.

Kozminski, K.G., P.L. Beech, and J.L. Rosenbaum. 1995. The *Chlamydomonas* kinesin-like protein FLA10 is involved in motility associated with the flagellar membrane. *J. Cell Biol.* 131:1517–1527.

LeCluyse, E.L., and W.L. Dentler. 1984. Asymmetric microtubule capping structures at the tips of frog palate cilia. *J. Ultrastruct. Res.* 86:75–85.

Lefebvre, P.A. 1995. Flagellar amputation and regeneration in *Chlamydomonas*. *Methods Cell Biol.* 47:3–7.

Lefebvre, P.A., and J.L. Rosenbaum. 1986. Regulation of the synthesis and assembly of ciliary and flagellar proteins during regeneration. *Annu. Rev. Cell Biol.* 2:517–546.

Lefebvre, P.A., S.A. Nordstrom, J.E. Moulder, and J.L. Rosenbaum. 1978. Flagellar elongation and shortening in *Chlamydomonas*. IV Effects of flagellar detachment, regeneration, and resorption on the induction of flagellar protein synthesis. *J. Cell Biol.* 78:8–27.

Marshall, W. 2002. Size control in dynamic organelles. *Trends Cell Biol.* 12: 414–419.

Marshall, W.F., and J.L. Rosenbaum. 2001. Intraflagellar transport balances continuous turnover of outer doublet microtubules: implications for flagellar length control. *J. Cell Biol.* 155:405–414.

Marshall, W.F., H. Qin, M.R. Brenni, and J.L. Rosenbaum. 2005. Flagellar length control system: testing a simple model based on intraflagellar transport and turnover. *Mol. Biol. Cell.* 16:270–278.

Matsuura, K., P.A. Lefebvre, R. Kamiya, and M. Hirono. 2002. Kinesin-II is not essential for mitosis and cell growth in *Chlamydomonas*. *Cell Motil. Cytoskeleton.* 52:195–201.

Mueller, J., C.A. Perrone, R. Bower, D.G. Cole, and M.E. Porter. 2005. The *FLA3* KAP subunit is required for localization of kinesin-2 to the site of flagellar assembly and processive anterograde intraflagellar transport. *Mol. Biol. Cell.* 16:1341–1354.

Nauli, S.M., F.J. Alenghat, Y. Luo, E. Williams, P. Vassilev, X. Li, A.E. Elia, W. Lu, E.M. Brown, S.J. Quinn, et al. 2003. Polycystins 1 and 2 mediate mechanosensation in the primary cilium of kidney cells. *Nat. Genet.* 33:129–137.

Nguyen, R.L., L.W. Tam, and P.A. Lefebvre. 2005. The LF1 gene of *Chlamydomonas reinhardtii* encodes a novel protein required for flagellar length control. *Genetics*. 169:1415–1424

Nonaka, S., Y. Tanaka, Y. Okada, S. Takeda, A. Harada, Y. Kanai, M. Kido, and N. Hirokawa. 1998. Randomization of left-right asymmetry due to loss of nodal cilia generating leftward flow of extraembryonic fluid in mice lacking KIF3B motor protein. *Cell.* 95:829–837.

Omoto, C.K., and G.B. Witman. 1981. Functionally significant central-pair rotation in a primitive eukaryotic flagellum. *Nature.* 290:708–710.

Pan, J., Q. Wang, and W.J. Snell. 2004. An aurora kinase is essential for flagellar disassembly in *Chlamydomonas*. *Dev. Cell.* 6:445–451.

Parker, J.D., and L.M. Quarmby. 2003. *Chlamydomonas* fla mutants reveal a link between deflagellation and intraflagellar transport. *BMC Cell Biol.* 4:11.

Pazour, G.J., and J.L. Rosenbaum. 2002. Intraflagellar transport and cilia-dependent diseases. *Trends Cell Biol.* 12:551–555.

Pazour, G.J., and G.B. Witman. 2003. The vertebrate primary cilium is a sensory organelle. *Curr. Opin. Cell Biol.* 15:105–110.

Pazour, G.J., C.G. Wilkerson, and G.B. Witman. 1998. A dynein light chain is essential for the retrograde particle movement of intraflagellar transport (IFT). *J. Cell Biol.* 141:979–992.

Pazour, G.J., B.L. Dickert, and G.B. Witman. 1999. The DHC1b (DHC2) isoform of cytoplasmic dynein is required for flagellar assembly. *J. Cell Biol.* 144:473–481.

Piperno, G., E. Siuda, S. Henderson, M. Segil, H. Vaananen, and M. Sassaroli. 1998. Distinct mutants of retrograde intraflagellar transport (IFT) share similar morphological and molecular defects. *J. Cell Biol.* 143:1591–1601.

Praetorius, H.A., J. Frokiaer, S. Nielsen, and K.R. Spring. 2003. Bending the primary cilium opens $Ca^{2+}$-sensitive intermediate-conductance $K^+$ channels in MCDK cells. *J. Membr. Biol.* 191:193–200.

Porter, M.E., R. Bower, J.A. Knott, P. Byrd, P., and W. Dentler. 1999. Cytoplasmic dynein heavy chain 1b is required for flagellar assembly in *Chlamydomonas*. *Mol. Biol. Cell.* 10:693–712.

Qin, H., D.F. Diener, S. Geimer, D.G. Cole, and J.L. Rosenbaum. 2004. Intraflagellar transport (IFT) cargo: IFT transports flagellar precursors to the tip and turnover products to the cell body. *J. Cell Biol.* 164:255–266.

Rosenbaum, J.L., and G.B. Witman. 2002. Intraflagellar transport. *Nat. Rev. Mol. Cell Biol.* 3:813–825.

Rosenbaum, J.L., J.E. Moulder, and D.L. Ringo. 1969. Flagellar elongation and shortening in *Chlamydomonas*. The use of cycloheximide and colchicine to study the synthesis and assembly of flagellar proteins. *J. Cell Biol.* 41:600–619.

Sager, R., and S. Granick. 1953. Nutritional studies with *Chlamydomonas reinhardtii*. *Ann. NY Acad. Sci.* 56:831–838.

Scholey, J.M. 2003. Intraflagellar transport. *Annu. Rev. Cell Dev. Biol.* 19:423–443.

Snell, W.J., J. Pan, and O. Wang. 2004. Cilia and flagella revealed: from flagellar assembly in *Chlamydomonas* to human obesity disorders. *Cell.* 117:693–697.

Snow, J.J., G. Ou, A.L. Gunnarson, M.R.S. Walker, H.M. Zhou, I. Brust-Mascher, and J.M. Scholey. 2004. Two anterograde intraflagellar transport motors cooperate to build sensory cilia on *C. elegans* neurons. *Nat. Cell Biol.* 6:1109–1113.

Song, L., and W.L. Dentler. 2001. Flagellar protein dynamics in *Chlamydomonas*. *J. Biol. Chem.* 276:29754–29763.

Stephens, R.E. 2000. Preferential incorporation of tubulin into the junctional region of ciliary outer doublet microtubules: a model for treadmilling by lattice dislocation. *Cell Motil. Cytoskeleton.* 47:130–140.

Tam, L.W., W.L. Dentler, and P.A. Lefebvre. 2003. Defective flagellar assembly and length regulation in LF3 null mutants in *Chlamydomonas*. *J. Cell Biol.* 163:597–607.

Tamm, S.L., and S. Tamm. 1988. Development of macrociliary cells in *Beroe*. II Formation of macrocilia. *J. Cell Sci.* 89:81–95.

Tuxhorn, J., T. Daise, and W.L. Dentler. 1998. Regulation of flagellar length in *Chlamydomonas*. *Cell Motil. Cytoskeleton.* 40:133–146.

Tyler, S. 1979. Distinctive features of cilia in metazoans and their significance for systematics. *Tissue Cell.* 11:385–400.

Walther, Z., M. Vashistha, and J.L. Hall. 1994. The *Chlamydomonas FLA10* gene encodes a novel kinesin-homologous protein. *J. Cell Biol.* 126:175–188.